Organic & Biomolecular Chemistry

PAPER

View Article Online
View Journal | View Issue

Published on 08 November 2013. Downloaded by St. Petersburg State University on 12/02/2014 16:18:01.

Cite this: *Org. Biomol. Chem.*, 2014, **12**, 998

Synthesis, and antibacterial activity of novel 4,5-dihydro-1*H*-pyrazole derivatives as DNA gyrase inhibitors

Jia-Jia Liu,† Juan Sun,† Yun-Bin Fang, Yong-An Yang,* Rui-Hua Jiao* and Hai-Liang Zhu*

Received 26th September 2013,
Accepted 8th November 2013

DOI: 10.1039/c3ob41953c

www.rsc.org/obc

A series of novel 4,5-dihydropyrazole derivatives (**4a–4t**), containing the dinitrobenzotrifluoride moiety, as DNA gyrase inhibitors were designed and synthesized. Based on the preliminary results, compounds **4d**, **4h** and **4t** with potent inhibitory activity in bacterial growth may be wonderful antibacterial agents; among them, compound **4t** displayed the most potent activity with minimum inhibitory concentration (MIC) values of 3.125, 0.39, 0.39 and 0.39 μg mL^{-1} against *Bacillus subtilis*, *Staphylococcus aureus*, *Pseudomonas aeruginosa*, and *Escherichia coli* respectively, which was comparable with penicillin and kanamycin B with corresponding MIC values of 3.125, 3.125, 0.39, 0.39 μg mL^{-1} and 1.562, 1.562, 1.562, 1.562 μg mL^{-1}, respectively. In particular, compound **4d** showed the most potent anti-Gram-positive bacterial activity with a MIC value of 0.39 μg mL^{-1} against the tested Gram-positive bacterial strains and exhibited the most potent *B. subtilis* DNA gyrase and *S. aureus* DNA gyrase inhibitory activity with an IC_{50} of 0.125 μg mL^{-1}. Docking simulation was performed to insert compound **4d** into the *S. aureus* DNA gyrase active site to determine the probable binding conformation.

1. Introduction

Bacterial infection remains a serious threat to human lives because of its emerging resistance to existing antibiotics, which is an increasing public health problem,[1] so the development and spread of antibiotic resistance among bacteria has become a major health and economic problem. The majority of antimicrobials are directed at a small group of well-validated targets, suggesting that these are the most effective ways to kill cells. As a result, research into these targets, either in the development of novel inhibitors or modification of existing agents, is very important for future drug development.[2]

DNA gyrase, a typical type II topoisomerase, has been known to cause DNA replication, transcription and recombination.[3] DNA gyrase catalyzes the ATP-dependent introduction of negative supercoils into bacterial DNA as well as the unknotting and deactivation of DNA.[4] DNA gyrase is mainly inhibited by coumarins and quinolones, some of which are widely used for the treatment of bacterial infectious diseases (*e.g.*, ciprooxacin).[5,6] DNA gyrase, consisting of the subunits GyrA and GyrB, is a member of the type II family of topoisomerases. GyrA is responsible for the DNA breakage and reunion that is necessary for negative supercoiling by DNA gyrase and normal DNA biosynthesis, whereas GyrB catalyzes the hydrolysis of ATP that provides the energy required to carry out enzyme function. Unfortunately, of late, multidrug-resistant Gram-positive bacteria have started posing medical science serious problems to deal with. To overcome the limitations of the known DNA gyrase inhibitors, it has become imperative and meaningful to identify new class of compounds.

Many pyrazole derivatives are well acknowledged to possess a wide range of antibacterial bioactivities.[7–10] Dihydropyrazole, a small bioactive molecule, is a prominent structural motif found in numerous pharmaceutically active compounds.[11] Among them, 4,5-dihydropyrazoles, as an important class of heterocyclic small molecules, are important biological agents with a wide range of pharmaceutical (antifungal, antibacterial, antitumor, anti-inflammatory, and antiviral) and agrochemical activities.[12–14] Liu *et al.* also discussed the synthesis, structure and antibacterial activity of new 2-(1-(2-(substituted-phenyl)-5-methyloxazol-4-yl)-3-(2-substituted-phenyl)-4,5-dihydro-1*H*-pyrazol-5-yl)-7-substituted-1,2,3,4-tetrahydroisoquinoline derivatives and found that two compounds of the series can strongly inhibit *Staphylococcus aureus* DNA gyrase (with IC_{50} values of 0.125 and 0.25 μg mL^{-1} against *S. aureus* DNA gyrase, 0.25 and 0.125 μg mL^{-1} against *Bacillus subtilis* DNA gyrase).[15]

State Key Laboratory of Pharmaceutical Biotechnology, Nanjing University, Nanjing 210093, People's Republic of China. E-mail: zhuhl@nju.edu.cn; Fax: +86 25 83592672; Tel: +86 25 83592672
† These two authors equally contributed to this paper.

This journal is © The Royal Society of Chemistry 2014

Published on 08 November 2013. Downloaded by St. Petersburg State University on 12/02/2014 16:18:01.

Much attention has always paid to pyrazole as a potential antimicrobial agent after the discovery of the natural pyrazole C-glycoside pyrazofurin which has shown a broad spectrum of antimicrobial activity.[16] Some pyrazole derivatives used as potent and selective inhibitors against DNA gyrase are capable of causing bacterial cell death, for example, the groups of Hoffmann-La Roche Ltd.[17,18] have developed a new lead DNA gyrase inhibitor (compound **1′**, Fig. 1).[15] Recently, Tanitame *et al.*[19] have identified an agent (compound **3′**, Fig. 2), which has been used as a potent and selective inhibitor against DNA gyrase capable of causing bacterial cell death. Moreover, our laboratory has recently published related pyrazole derivatives as DNA gyrase inhibitors.[20] Many selective inhibitors of DNA gyrase shown in Fig. 2 contain aryl-pyrazole template. The trifluoromethyl-substituted compounds have also been reported to possess biological activities and are often employed as fungicides,[21] antipyretic agents[22] and analgesic[23] agents.

In view of the above-mentioned findings, we report in the present work the synthesis of a series of pyrazole derivatives to extend the research to achieve new potential antibacterial DNA gyrase inhibitors by structural optimization. The trifluoromethyl-substituted moiety was introduced to enhance the molecular interactions, which are based on the results of CADD (computer-assisted drug design). With the trifluoromethyl-substituted moiety fixed, we introduced different substituents on the A-ring and B-ring (see later in Table 1) to study the structure–activity relationships in antibacterial activity for further optimization. Thus we studied their antimicrobial activities and DNA gyrase inhibitory activities. Docking simulations were performed using the X-ray crystallographic

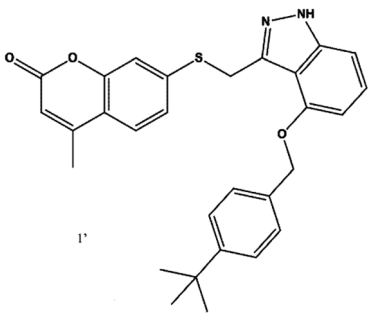

Fig. 1 A new lead DNA gyrase inhibitor developed by groups at Hoffmann-La Roche Ltd.

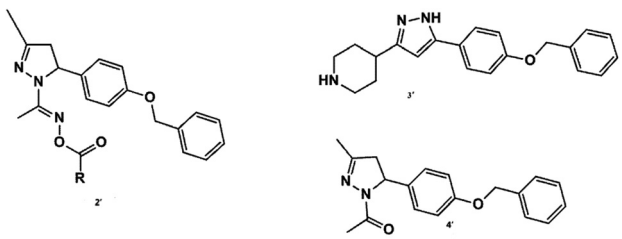

Fig. 2 Recently disclosed pyrazole as antibacterial inhibitors.

Table 1 Chemical structures of **4a–4t**

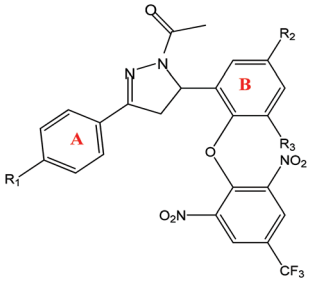

Compound	R_1	R_3	R_2
4a	CH_3	Br	Br
4b	CH_3	Cl	Cl
4c	CH_3	H	Br
4d	CH_3	H	Cl
4e	OCH_3	Br	Br
4f	OCH_3	Cl	Cl
4g	OCH_3	H	Br
4h	OCH_3	H	Cl
4i	F	Br	Br
4j	F	Cl	Cl
4k	F	H	Br
4l	F	H	Cl
4m	Cl	Br	Br
4n	Cl	Cl	Cl
4o	Cl	H	Br
4p	Cl	H	Cl
4q	Br	Br	Br
4r	Br	Cl	Cl
4s	Br	H	Br
4t	Br	H	Cl

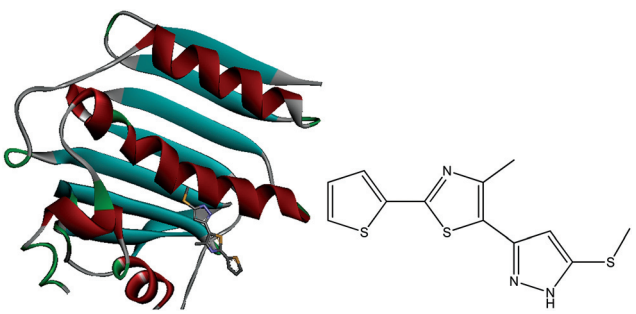

Fig. 3 Crystal structure of *S. aureus* gyrase B co-complexed with inhibitor.

structure of the DNA gyrase of *S. aureus*, which is shown in Fig. 3,[24] in complex with the most potent inhibitor to explore the binding model of the compound at the active site.

2. Results and discussion

2.1. Chemistry

The synthesis of compounds (**4a–4t**) followed the general pathway outlined in Scheme 1 and the structures of these compounds are shown in Table 1. Compounds (**4a–4t**) were prepared in four steps. Firstly, the chalcones (**1a–1t**) were

Published on 08 November 2013. Downloaded by St. Petersburg State University on 12/02/2014 16:18:01.

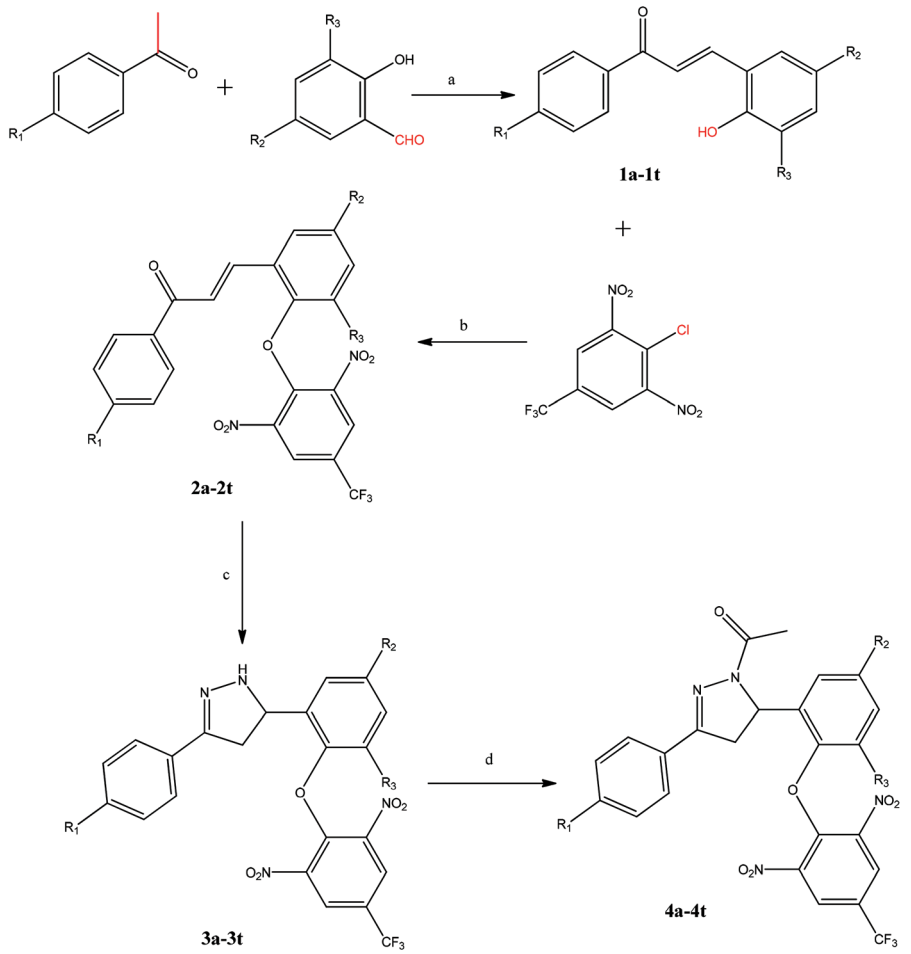

Scheme 1 The synthetic routes of compounds **4a–4t**. *Reagents and conditions*: (a) ethanol, NaOH, rt, 4–6 h; (b) DMF, potassium *tert*-butoxide, rt, 4 h; (c) $NH_2{\cdot}NH_2{\cdot}H_2O$, EtOH, 80 °C; (d) EDC·HCl, CH_2Cl_2, rt.

obtained *via* the substituted salicylaldehydes and substituted acetophenones, using 40% sodium hydroxide as catalyst in ethanol. Secondly, chalcones (**1a–1t**), 4-chloro-3,5-dinitro-α,α,α-trifluorotoluene and potassium *tert*-butoxide were dissolved in DMF and reacted to obtain the desired compounds (**2a–2t**) at the room temperature. Thirdly, treating chalcone derivatives in refluxing ethanol with hydrazine hydrate for 8 h produced the desired compounds (**3a–3t**). Finally, to a solution of compounds (**3a–3t**) respectively in dichloromethane, acetic acid derivatives were added, together with EDC·HCl (1-ethyl-3-(3-dimethylaminopropyl)carbodiimide) and HOBt (hydroxybenzotriazole). The mixture was refluxed under stirring for 8 h to obtain the desired compounds (**4a–4t**). All the synthetic compounds were characterized by ^{1}H NMR, elemental analysis and mass spectrometry, the results of which were in full accordance with their depicted structures.

2.2. Biological activity

2.2.1. Antibacterial activity. The antibacterial activities of the synthetic compounds were tested against two Gram-negative bacterial strains: *Escherichia coli* ATCC 25922 and *Pseudomonas aeruginosa* ATCC 27853, and against two Gram-positive bacterial strains: *B. subtilis* ATCC 530 and *S. aureus* ATCC 25923, using the method recommended by National Committee for Clinical Laboratory Standards (NCCLS).[25,26]

The MIC (minimum inhibitory concentration) values of those compounds against these bacteria are presented in Table 2. Penicillin and standard antibacterial agent kanamycin B were also screened under identical conditions for comparison. The results revealed that most of the synthetic compounds exhibited significant antibacterial activities.

Out of the 20 pyrazole derivatives, compound **4t** displayed broad-spectrum antimicrobial activity against all tested bacterial strains (*E. coli*, *P. aeruginosa*, *S. aureus* and *B. subtilis*) with MIC values of 0.39–3.125 μg mL^{-1}; it also displayed the most potent activity with MIC values of 3.125, 0.39, 0.39 and 0.39 μg mL^{-1} against *B. subtilis*, *S. aureus*, *P. aeruginosa*, *E. coli* respectively, which was comparable with penicillin and kanamycin B with corresponding MIC values of 3.125, 3.125, 0.39, 0.39 μg mL^{-1} and 1.562, 1.562, 1.562, 1.562 μg mL^{-1}, respectively. Moreover, compound **4d** showed the most potent activity with MIC values of 0.39 and 0.39 μg mL^{-1} against *B. subtilis*,

 This journal is © The Royal Society of Chemistry 2014

Published on 08 November 2013. Downloaded by St. Petersburg State University on 12/02/2014 16:18:01.

Table 2 Antimicrobial activity of the synthesized compounds

	Minimum inhibitory concentration/μg mL^{-1}			
	Gram-positive		Gram-negative	
Compound	*B. subtilis*	*S. aureus*	*P. aeruginosa*	*E. coli*
4a	3.125	3.125	6.25	1.562
4b	6.25	25	6.25	3.125
4c	6.25	6.25	3.125	1.562
4d	0.39	0.39	1.562	12.5
4e	3.125	6.25	6.25	6.25
4f	3.125	6.25	6.25	3.125
4g	3.125	1.562	3.125	1.562
4h	3.125	1.562	0.39	0.39
4i	1.562	12.5	12.5	6.25
4j	6.25	12.5	6.25	3.125
4k	12.5	6.25	3.125	1.562
4l	50	12.5	0.39	3.125
4m	3.125	6.25	1.562	6.25
4n	6.25	3.125	1.562	3.125
4o	1.562	3.125	3.125	1.562
4p	1.562	3.125	1.562	3.125
4q	3.125	6.25	1.562	1.562
4r	25	50	6.25	3.125
4s	3.125	3.125	3.125	1.562
4t	3.125	0.39	0.39	0.39
Penicillin	3.125	3.125	0.39	0.39
Kanamycin B	1.562	1.562	1.562	1.562

S. aureus and compound **4h** and **4t** both showed the most potent activity with MIC values of 0.39 and 0.39 μg mL^{-1} against *P. aeruginosa*, *E. coli* respectively.

Subsequently structure–activity relationship (SAR) studies were performed to determine how the substituents on the benzene ring affected the antimicrobial activity. Firstly, structure–activity relationships in these dihydropyrazole derivatives displayed that compounds with *para* electron-donating substituents (**4a–4h**) on the A-ring showed more potent activities than those with electron-withdrawing substituents (**4i–4t**) on the A-ring. Substituents F (**4i–4l**), Cl (**4m–4p**) and Br (**4q–4t**), compared with CH_3 (**4a–4d**) and OCH_3 (**4e–4h**), mostly had moderate effects, which is clearly seen in Table 2.

Secondly, in the case of a constant A-ring substituent, a change of substituent on the B-ring could also affect the activities of these compounds. It can be found that compounds with a halogen atom on the 5-position of the salicylaldehyde mostly displayed a higher antibacterial activity than compounds with two halogen atoms at both the 3- and 5-positions of the salicylaldehyde. Among compounds with a halogen atom at the 5-position of the salicylaldehyde, mostly, the strength order is Cl > Br. Thus, compounds **4d** and **4h** with a *para* electron-donating group in the A-ring and Cl in the B-ring both showed a wonderful antibacterial activity.

Finally, we view the bioassay from Table 2 and found that, on one hand, the bioassay of the Gram-positive bacteria shows that the strength order is CH_3 > OCH_3 for compounds with a *para* electron-donating substituent (**4a–4h**) on the A-ring and the strength order is Cl > Br > F for compounds with an electron-withdrawing substituent (**4i–4t**) on the A-ring; on the other hand, the bioassay of the Gram-negative bacteria also shows the strength order is OCH_3 > CH_3 for compounds with a *para* electron-donating substituent (**4a–4h**) on the A-ring and the strength order is Br > Cl > F for compounds with an electron-withdrawing substituent (**4i–4t**) on the A-ring. Thus, compound **4d** with *para*-CH_3 group on the A-ring and Cl on the B-ring showed the best anti-Gram-positive activity. The compound **4h** with the *para*-OCH_3 group on the A-ring and Cl on the B-ring and **4t** with Br on the A-ring and Cl on the B-ring both showed the best anti-Gram-negative activity.

Next, we chose some of the selected compounds to test Gram-positive inhibitory activities rather than Gram-negative inhibitory activities. Of late, the number of reported Gram-positive inhibitors is fewer than for Gram-negative inhibitors, and the multidrug-resistant Gram-positive bacteria have started posing serious problems to be dealt with in medical science, so research about the Gram-positive inhibitors is more meaningful and interesting.

2.2.2. *B. subtilis* DNA gyrase and *S. aureus* DNA gyrase inhibitory activity. In addition, to elucidate the mechanism by which the pyrazole derivatives induce anti-Gram-positive bacterial activity, the inhibitory activities of the selected 8 compounds (**4a**, **4d**, **4g**, **4h**, **4o**, **4p**, **4s**, and **4t**) and the bottom 3 compounds (**4b**, **4l** and **4r**) were examined against DNA gyrase isolated from *B. subtilis* and *S. aureus*. As shown in Table 3, all the bottom compounds showed poor DNA gyrase inhibitory activities whereas most of the top compounds displayed potent DNA gyrase inhibitory activities. Among the tested compounds, compound **4d** with potent anti-Gram-positive bacterial activity strongly inhibited *B. subtilis* DNA gyrase and *S. aureus* DNA gyrase (with an IC_{50} of 0.125 μg mL^{-1} against *B. subtilis* DNA gyrase, and 0.125 μg mL^{-1} against *S. aureus* DNA gyrase), which is comparable to the positive control Novobiocin with an IC_{50} of 0.5 μg mL^{-1} against *B. subtilis* DNA gyrase and 0.25 μg mL^{-1} against *S. aureus* DNA gyrase. Other tested top compounds displayed good inhibitory activity with IC_{50} values ranging from 0.125 to 1.0 μg mL^{-1}, whereas the IC_{50} results of the bottom 3 compounds were all >1.0 μg mL^{-1}. The results indicated that **4d** had a high binding affinity with DNA gyrase, which supported the potent anti-Gram-positive

Table 3 Inhibitory effects of the selected compounds against DNA gyrase[a]

	IC_{50}/μg mL^{-1}	
Compound	*S. aureus* DNA gyrase	*B. subtilis* DNA gyrase
4a	0.5	0.5
4b	>1.0	>1.0
4d	0.125	0.125
4g	0.5	0.5
4h	0.5	0.5
4l	>1.0	>1.0
4o	0.25	0.5
4p	0.25	0.5
4r	>1.0	>1.0
4s	0.5	0.5
4t	0.125	0.25
Novobiocin	0.25	0.5

[a] DNA gyrase supercoiling activity.

Published on 08 November 2013. Downloaded by St. Petersburg State University on 12/02/2014 16:18:01.

Table 4 Hemolytic activities and cytotoxicity of the selected compounds

Compounds	Hemolysis LC_{30} [a]/mg mL^{-1}	Cytotoxicity IC_{50}/μM	Bodyweight/g ± SD	
			0 days	7 days
4a	>10	193.1	21.65 ± 1.09	25.11 ± 1.86
4b	>10	235.3	21.12 ± 0.98	25.45 ± 1.43
4d	>10	130.4	22.09 ± 1.56	27.09 ± 0.93
4g	>10	182.6	21.11 ± 2.34	25.34 ± 1.15
4h	>10	173.7	20.57 ± 1.43	26.75 ± 1.56
4l	>10	240.4	24.32 ± 1.11	25.53 ± 1.98
4o	>10	163.6	21.59 ± 1.90	23.64 ± 2.54
4p	>10	150.5	21.33 ± 0.67	25.83 ± 1.33
4o	>10	155.6	20.78 ± 1.03	25.25 ± 1.76
4r	>10	252.3	21.43 ± 1.22	21.08 ± 2.00
4t	>10	140.5	22.18 ± 2.15	27.57 ± 1.56
DDCP	>10	125.6	21.87 ± 0.78	25.37 ± 1.23

[a] Lytic concentration 30%.

bacterial activity of **4d**, and that the bottom 3 compounds (**4b**, **4l** and **4r**) had a low binding affinity with DNA gyrase, which also supported the moderate anti-Gram-positive bacterial activity of **4b**, **4l** and **4r**. The results of *B. subtilis* DNA gyrase and *S. aureus* DNA gyrase inhibitory activities of the test compounds corresponded to the structure–activity relationships (SAR) of their anti-Gram-negative bacterial activities. This demonstrated that the potent anti-Gram-positive bacterial activities of the synthetic compounds were probably correlated to their related DNA gyrase inhibitory activities.

2.2.3. Acute oral toxicity. Five thousand milligrams of compounds **4d**, **4h** and **4t** per kilogram of bodyweight was administered to ten healthy rats by oral gavage. The animals were observed for mortality, signs of gross toxicity and behavioral changes at least once daily for 14 days. Bodyweights were recorded prior to administration and again on day 7 and 14. All animals survived and appeared active and healthy throughout the study. With the exception of one male that exhibited a loss in bodyweight between day 7 and 14, all animals gained bodyweight over the 14-day observation period. There were no signs of gross toxicity or abnormal behavior. Acute oral toxicity was tested according to OECD guideline 423. All experimental protocols and animal care complied with the Guide for the Care and Use of Laboratory Animals, Institute of Laboratory Animal Resources, and were approved by the Institutional Animal Care and Use Committee of Nanjing Medical College. The acute oral toxicity tests were run in accordance with the guide of biological evaluation of medical device (CFDA, China).

2.2.4. Cytotoxicity test. In order to find potent antibiotics, it is important to measure their cytotoxicity. One of the major hindrances to the clinical use of many compounds with effective antibacterial activities, however, is their ability to damage mammalian cell that leads to high hemolytic and cytotoxic activity dangerous to the host organism. Hemolytic activity is conventionally used as a measure of cytotoxicity and as a model for mammalian cells because red blood cells are, in general, extremely fragile. However, sometimes, compounds that show low hemolytic activities have the severe cytotoxicity against mammalian cells. So the hemolysis and cytotoxicity assays were both undertaken.

The compounds selected above were also detected for their hemolytic activity. Then we further tested their cytotoxic activity on a mouse embryonic fibroblast cell line (NIH-3T3) using the MTT assay to prove the potency of the compounds.[27]

The pharmacological results of these compounds are summarized in Table 4. It can be seen from Table 4 that the selected compounds displayed low hemolytic activities. Besides, the cytotoxicity assay determined the selectivity of our compounds for bacterial over mammalian cells. What we can see from the data is that the compounds with potent inhibitory activity showed low toxicity which is comparable to the positive control DDCP (dichloro-1,2-dithiacyclopentenone).[28]

2.3. Binding model of DNA gyrase

Molecular docking is an application wherein molecular modeling techniques are used to predict how a protein (enzyme) interacts with small molecules (ligands).[29] In the present study, to understand the interactions between compounds and BRAF and to explore their binding mode, a docking study was performed using the CDOCKER protocol in Discovery Studio 3.1 (Discovery Studio 3.1, Accelrys, Inc., San Diego, CA).

To gain better understanding on the potency of compounds **4d**, **4h**, **4t** and guide further SAR studies, the molecular docking of all the synthetic acylhydrazone derivatives and DNA gyrase was performed on the binding model based on the DNA gyrase complex structure (3G75.pdb) by using the Discovery Studio (version 3.1).

Our compounds had a good binding affinity for DNA gyrase and the results of EDOCKER_ENERGY almost have the same trend with the structure–activity relationships of antibacterial activities, which further confirmed the correlation between the antibacterial activities and DNA gyrase inhibitory activities of our compounds.

Among them, compound **4t** with the most potent inhibitory activity showed the minimum data, which suggested that it was mostly easy to combine with DNA gyrase. The binding model of compound **4t** with 3G75 is depicted in Fig. 4. In the binding model of **4t**, **4t** is nicely bound to the 3G75 *via* two hydrogen bonds with Ser 55 (H–O···H: 2.46 Å, 101.42°), Thr 173 (H–O···H: 2.18 Å, 147.32°) and three ionic bonds with

 This journal is © The Royal Society of Chemistry 2014

Published on 08 November 2013. Downloaded by St. Petersburg State University on 12/02/2014 16:18:01.

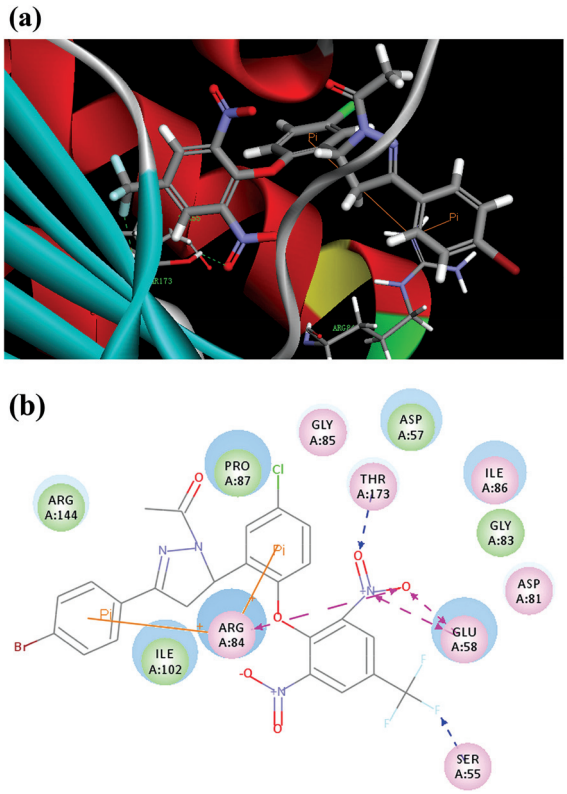

Fig. 4 (a) Compound **4t** (colored by atom: carbon, gray; nitrogen, blue; oxygen, red; sulfur, yellow) is bonding into DNA gyrase. The dotted lines show the hydrogen bonding. (b) 2D ligand interaction diagram of compound **4t** with DNA gyrase using the Discovery Studio program where the essential amino acid residues at the binding site are tagged in circles. The purple circles show the amino acids which participate in hydrogen bonding, electrostatic or polar interactions and the green circles show the amino acids which participate in the van der Waals interactions.

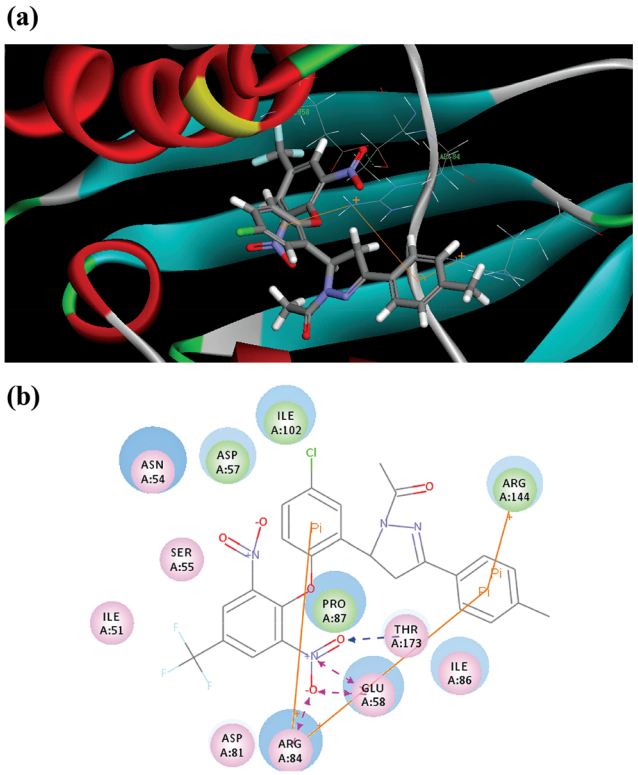

Fig. 5 (a) Compound **4h** (colored by atom: carbon, gray; nitrogen, blue; oxygen, red; sulfur, yellow) is bonding into DNA gyrase. The dotted lines show the hydrogen bonding. (b) 2D ligand interaction diagram of compound **4h** with DNA gyrase using the Discovery Studio program where the essential amino acid residues at the binding site are tagged in circles. The purple circles show the amino acids which participate in hydrogen bonding, electrostatic or polar interactions and the green circles show the amino acids which participate in the van der Waals interactions.

Glu 58 (N–O···H: 2.6 Å), (O···H: 2.8 Å), and Arg 84 (O···H: 3.9 Å), which enhance the binding affinity, resulting in the increased antimicrobial activity of this compound. Therefore, high binding affinities resulted in strong antimicrobial activity and the initial attempt to achieve a new potential antibacterial DNA gyrase inhibitor has been verified with the expected results. Also Arg 84 plays an important role in the complex involving π–π interaction (distance = 4.1 Å) with the A-ring and π–π interactions (distance = 5.5 Å) with the B-ring of the 4,5-dihydropyrazole core, which shares the same interaction method of DNA gyrase.

In the binding model, compound **4h** with the most potent anti-Gram-negative bacterial inhibitory activity showed the minimum data, which suggested that it was easy to combine with DNA gyrase, as is shown in Fig. 5, which is nicely bound to 3G75 *via* one hydrogen bond, three π–π interactions and three ionic bonds. One oxygen atom of the dinitrobenzotrifluoride moiety contributes to the hydrogen bonding interaction (O···H–N: 2.02 Å, 138.991°) with the backbone amino hydrogen atom of Thr 173. Meanwhile, the nitro-group of the dinitrobenzotrifluoride moiety has formed ionic bonds together with Glu 58 and Arg 84, which suggests that the introduction of the dinitrobenzotrifluoride moiety has enhanced the combination of the receptor and ligand. Further, the B-ring and A-ring of compound **4h** both form a π–π interaction with Arg 84 and the A-ring of compound **4h** also form a π–π interaction with Arg 144. This ensures the binding affinity and results in an increased DNA gyrase inhibitory activity.

Compound **4d** with the most potent anti-Gram-positive bacterial inhibitory activity showed the minimum data, which suggested that it was also easy to combine with DNA gyrase. The binding model of compound **4d** with 3G75 is depicted in Fig. 6. In the binding model of **4d**, **4d** is nicely bound to 3G75 *via* one hydrogen bond with Thr 173 (H–O···H: 2.13 Å, 148.99°) and three ionic bonds with Glu 58 (N–O···H: 2.6 Å), (O···H: 2.9 Å), and Arg 84 (O···H: 3.9 Å), which enhance the binding affinity, resulting in the increased antimicrobial activity of this compound. Therefore, high binding affinities resulted in strong antimicrobial activity and the initial attempt to achieve a new potential antibacterial DNA gyrase inhibitor has been verified with the expected results. Also, Arg 84 plays an important role in the complex involving a π–π interaction (distance = 4.7 Å) with the A-ring and π–π interactions (distance = 5.4 Å) with the B-ring of the 4,5-dihydropyrazole core, which shares the same

Published on 08 November 2013. Downloaded by St. Petersburg State University on 12/02/2014 16:18:01.

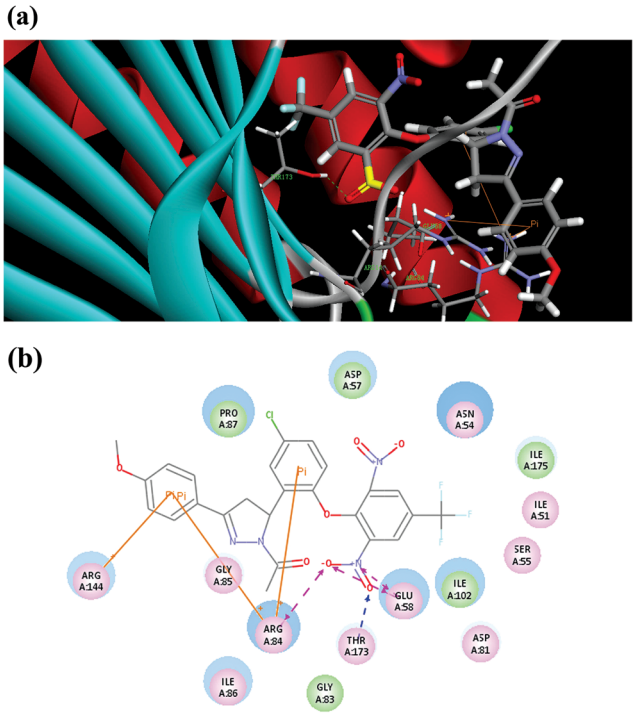

Fig. 6 (a) Compound **4d** (colored by atom: carbon, gray; nitrogen, blue; oxygen, red; sulfur, yellow) is bonding to DNA gyrase. The dotted lines show the hydrogen bonding. (b) 2D ligand interaction diagram of compound **4d** with DNA gyrase using the Discovery Studio program where the essential amino acid residues at the binding site are tagged in circles. The purple circles show the amino acids which participate in hydrogen bonding, electrostatic or polar interactions and the green circles show the amino acids which participate in the van der Waals interactions.

interaction method of DNA gyrase, and the A-ring of compound **4d** also forms a π–π interaction with Arg 144 (distance = 4.6 Å).

3. Conclusion

In summary, a series of novel compounds containing the 4,5-dihydropyrazole core with a dinitrobenzotrifluoride moiety have been synthesized and evaluated for their antibacterial activity against *E. coli* ATCC 25922, *P. aeruginosa* ATCC 27853, *B. subtilis* ATCC 530 and *S. aureus* ATCC 25923 in order to achieve new and better potential antibacterial DNA gyrase inhibitors. Out of the 20 vanillic pyrazole derivatives, **4t** showed the most potent antibacterial activity with MIC values of 0.39–3.125 μg mL^{-1} against the tested bacterial strains and exhibited the good potent DNA gyrase inhibitory activity with IC_{50} values of 0.125–0.25 μg mL^{-1}. Moreover, compound **4d** and **4h** also showed strong antibacterial activity wjocj was proven by their nice DNA gyrase inhibitory activity with IC_{50}. Preliminary structure–activity relationships and molecular modeling studies provided further insight into the interactions between the enzyme and its ligands. All in all, this study showed that **4t**, **4h** and **4d** were novel compounds that could be potent antimicrobial inhibitors of DNA gyrase and have provided valuable information for the design of DNA gyrase inhibitors as antibacterial agents.

4. Experimental section

4.1. Materials and measurements

All chemicals (reagent grade) used were commercially available. Separation of the compounds by column chromatography was carried out with silica gel 60 (200–300 mesh ASTM, E. Merck, Germany). Developed plates were visualized using a Spectroline ENF 260C/F UV apparatus. The quantity of silica gel used was 50–100 times the weight charged on the column. Thin layer chromatography (TLC) was run on the silica gel-coated aluminum sheets (silica gel 60 GF254, E. Merck, Germany) and visualized under ultraviolet (UV) light (254 nm). The concentration and evaporation of the solvent after reaction or extraction were carried out using a rotary evaporator (Büchi Rotavapor) operating at reduced pressure. Melting points were measured using Boetius micro melting point apparatus. All of the proton nuclear magnetic resonance (^{1}H NMR) spectra were recorded using a DPX300 model spectrometer at 25 °C with TMS and solvent signals allotted as internal stands. Chemical shifts were reported in parts per million (ppm, d units). ESI-MS spectra were recorded using a Mariner System 5304 mass spectrometer. Elemental analyses were performed using a CHN-O-Rapid instrument and were within 0.4% of the theoretical values.

4.2. General procedure for synthesis of chalcones (1a–1t)

Equimolar portions of the appropriately substituted salicylaldehydes (2 mmol, 1 equiv.) and substituted acetophenone (2 mmol, 1 equiv.) were dissolved in approximately 10 mL of ethanol. The mixture was allowed to stir for several minutes at 0 °C to allow the reagents to dissolve. Then, a 0.5 mL aliquot of a 40% aqueous sodium hydroxide solution was slowly added dropwise to the reaction flask *via* a self-equalizing addition funnel. The reaction solution was allowed to stir at room temperature for approximately 4–6 h. The mixture was adjusted to pH 4.0 with dilute hydrochloric acid until the reaction was complete. The reaction was monitored by TLC. Mostly, a precipitate formed and was then collected by suction filtration.

4.3. General procedure for synthesis of target compounds (2a–2t)

A mixture of chalcones (**1a–1t**) (1 mmol), 4-chloro-3,5-dinitro-α,α,α-trifluorotoluene (**2**) (1 mmol) and potassium *tert*-butoxide (0.75 mmol) was dissolved in DMF and stirred at room temperature for 5 h. The products were extracted with ethyl acetate and water. The extracts were dried over anhydrous Na_2SO_4, filtered and evaporated. The residue was purified by column chromatography using petroleum ether and ethyl acetate (3 : 1).

4.4. General method of synthesis of 3,5-diphenyl-4,5-dihydro-1*H*-pyrazole (3a–3t)

To a solution of chalcone derivative (1 mmol) in isopropanol (5 mL), hydrazine hydrate (0.2 mL, 4 mmol) was added. The

 This journal is © The Royal Society of Chemistry 2014

Published on 08 November 2013. Downloaded by St. Petersburg State University on 12/02/2014 16:18:01.

mixture was refluxed under stirring for 8 h, stored at 4–5 °C for 24 h, and the precipitate formed was filtered off, then washed with cool ethanol. The synthesized compound was purified by crystallization from ethanol in a refrigerator and allowed to air-dry to obtain the 4,5-dihydropyrazole derivatives.

4.5. General method of synthesis of compounds (4a–4t)

To a solution of pyrazoline derivatives (1 mmol) in dichloromethane (5 mL) acetic acid (5 mL) was added, together with EDC (1.2–1.5 mmol) and HOBt (1.2–1.5 mmol). The mixture was refluxed under stirring for 8 h. After completion of the reaction, the contents were cooled, and then evaporated to dryness *in vacuo*. Aqueous hydrochloric acid (0.1 M, 30 mL) was added and the mixture extracted with ethyl acetate (3 × 5 mL). The combined ethyl acetate layers were back-extracted with saturated sodium bicarbonate (3 × 5 mL) and brine (3 × 5 mL), dried over $MgSO_4$, filtered, and evaporated *in vacuo*. The residue was crystallized from ethanol to obtain the target compounds.

4.5.1. (*E*)1-(5-(3,5-Dibromo-2-(2,6-dinitro-4-(trifluoromethyl)-phenoxy)phenyl)-3-(*p*-tolyl)-4,5-dihydro-1*H*-pyrazol-1-yl)ethanone (4a). White solid, mp: 203–205 °C. ^{1}H NMR (300 MHz, DMSO) δ: 1.98 (s, 3H), 2.33 (d, J = 6.42 Hz, 3H), 3.76–3.83 (m, 1H), 3.99–4.06 (m, 2H), 5.64–5.69 (m, 1H), 7.00 (d, J = 2.19 Hz, 1H), 7.30 (t, J = 8.78 Hz, 2H), 7.65 (t, J = 6.30 Hz, 1H), 7.80–7.85 (m, 2H), 9.85 (s, 1H), MS (ESI): 685 ($C_{25}H_{18}Br_2F_3N_4O_6$, $[M + H]^+$). Anal $C_{25}H_{17}Br_2F_3N_4O_6$. Calcd for: C, 43.76; H, 2.50; N, 8.16. Found: C, 43.68; H, 2.45; N, 8.21%.

4.5.2. (*E*)1-(5-(3,5-Dichloro-2-(2,6-dinitro-4-(trifluoromethyl)-phenoxy)phenyl)-3-(*p*-tolyl)-4,5-dihydro-1*H*-pyrazol-1-yl)ethanone (4b). White solid, mp: 245–247 °C. ^{1}H NMR (300 MHz, DMSO) δ: 2.00 (s, 3H), 2.50 (t, J = 1.83 Hz, 3H), 3.40 (s, 1H), 4.42 (J = 4.56 Hz, 2H), 5.66 (m, 1H), 7.57–7.64 (m, 3H), 7.74–7.78 (m, 1H), 8.28 (m, 1H), 11.98 (m, 1H), 12.40 (s, 1H), MS (ESI): 597 ($C_{25}H_{18}Cl_2F_3N_4O_6$, $[M + H]^+$). Anal $C_{25}H_{17}Cl_2F_3N_4O_6$. Calcd for: C, 50.27; H, 2.87; N, 9.38. Found: C, 49.98; H, 2.85; N, 9.31%.

4.5.3. (*E*)1-(5-(5-Bromo-2-(2,6-dinitro-4-(trifluoromethyl)-phenoxy)phenyl)-3-(*p*-tolyl)-4,5-dihydro-1*H*-pyrazol-1-yl)ethanone (4c). White solid, mp: 245–247 °C. ^{1}H NMR (300 MHz, DMSO) δ: 1.98 (s, 3H), 2.32 (d, J = 7.14 Hz, 3H), 3.72–3.82 (m, 1H), 3.99–4.06 (m, 2H), 5.54–5.59 (m, 1H), 6.79 (d, J = 8.61 Hz, 1H), 6.91 (d, J = 2.01 Hz, 1H), 7.21–7.26 (m, 3H), 7.65 (d, J = 7.86 Hz, 2H), 9.99 (s, 1H), MS (ESI): 607 ($C_{25}H_{19}BrF_3N_4O_6$, $[M + H]^+$). Anal $C_{25}H_{18}BrF_3N_4O_6$. Calcd for: C, 49.44; H, 2.99; N, 9.23. Found: C, 49.38; H, 2.95; N, 9.21%.

4.5.4. (*E*)1-(5-(5-Chloro-2-(2,6-dinitro-4-(trifluoromethyl)-phenoxy)phenyl)-3-(*p*-tolyl)-4,5-dihydro-1*H*-pyrazol-1-yl)ethanone (4d). White solid, mp: 260–262 °C. ^{1}H NMR (300 MHz, DMSO) δ: 1.99 (s, 3H), 2.35 (d, J = 2.04 Hz, 3H), 3.72–3.82 (m, 1H), 3.99–4.06 (m, 2H), 5.54–5.59 (m, 1H), 6.87 (d, J = 3.69 Hz, 1H), 6.96 (d, J = 2.01 Hz, 1H), 7.24 (s, 3H), 7.69 (d, J = 2.07 Hz, 2H), 9.93 (s, 1H), MS (ESI): 563 ($C_{25}H_{19}ClF_3N_4O_6$, $[M + H]^+$). Anal $C_{25}H_{18}ClF_3N_4O_6$. Calcd for: C, 53.34; H, 3.22; N, 9.95. Found: C, 53.38; H, 3.19; N, 9.91%.

4.5.5. (*E*)1-(5-(3,5-Dibromo-2-(2,6-dinitro-4-(trifluoromethyl)-phenoxy)phenyl)-3-(4-methoxyphenyl)-4,5-dihydro-1*H*-pyrazol-1-yl)ethanone (4e). White solid, mp: 245–247 °C. ^{1}H NMR (300 MHz, DMSO) δ: 2.50 (s, 3H), 3.58–3.61 (m, 3H), 3.93 (d, J = 2.04 Hz, 3H), 5.68 (d, J = 6.93 Hz, 1H), 7.01 (d, J = 2.19 Hz, 1H), 7.31 (t, J = 2.01 Hz, 2H), 7.65 (d, J = 2.19 Hz, 1H), 7.83 (t, J = 7.13 Hz, 2H), 9.79 (s, 1H), MS (ESI): 701 ($C_{25}H_{18}Br_2F_3N_4O_6$, $[M + H]^+$). Anal $C_{25}H_{17}Br_2F_3N_4O_6$. Calcd for: C, 42.76; H, 2.44; N, 7.98. Found: C, 42.58; H, 2.29; N, 7.91%.

4.5.6. (*E*)1-(5-(3,5-Dichloro-2-(2,6-dinitro-4-(trifluoromethyl)-phenoxy)phenyl)-3-(4-methoxyphenyl)-4,5-dihydro-1*H*-pyrazol-1-yl)ethanone (4f). White solid, mp: 198–200 °C. ^{1}H NMR (300 MHz, DMSO) δ: 2.19 (s, 3H), 3.45 (d, J = 2.04 Hz, 4H), 4.33 (s, 2H), 7.61 (d, J = 2.19 Hz, 1H), 7.78 (t, J = 2.01 Hz, 2H), 8.16–8.26 (m, 2H), 10.92 (s, 2H), 11.52 (d, J = 12.78 Hz, 1H), MS (ESI): 701 ($C_{25}H_{18}Cl_2F_3N_4O_6$, $[M + H]^+$). Anal $C_{25}H_{17}Cl_2F_3N_4O_6$. Calcd for: C, 48.96; H, 2.79; N, 9.13. Found: C, 48.88; H, 2.72; N, 9.11%.

4.5.7. (*E*)1-(5-(5-Bromo-2-(2,6-dinitro-4-(trifluoromethyl)-phenoxy)phenyl)-3-(4-methoxyphenyl)-4,5-dihydro-1*H*-pyrazol-1-yl)ethanone (4g). White solid, mp: 245–247 °C. ^{1}H NMR (300 MHz, DMSO) δ: 2.28 (s, 3H), 3.75 (d, J = 12.06 Hz, 4H), 3.97–4.06 (m, 2H), 5.51–5.56 (m, 1H), 6.77 (d, J = 8.61 Hz, 1H), 6.88 (s, 1H), 6.97 (d, J = 8.79 Hz, 2H), 7.18–7.22 (m, 1H), 7.67 (d, J = 8.79 Hz, 2H), 9.96 (s, 1H), MS (ESI): 701 ($C_{25}H_{19}BrF_3N_4O_7$, $[M + H]^+$). Anal $C_{25}H_{18}BrF_3N_4O_7$. Calcd for: C, 48.17; H, 2.91; N, 8.99. Found: C, 48.28; H, 2.92; N, 9.11%.

4.5.8. (*E*)1-(5-(5-Chloro-2-(2,6-dinitro-4-(trifluoromethyl)-phenoxy)phenyl)-3-(4-methoxyphenyl)-4,5-dihydro-1*H*-pyrazol-1-yl)ethanone (4h). White solid, mp: 255–257 °C. ^{1}H NMR (300 MHz, DMSO) δ: 2.34 (d, J = 18.84 Hz, 3H), 3.76 (t, J = 10.98 Hz, 4H), 3.99 (s, 2H), 5.56 (d, J = 7.68 Hz, 1H), 6.82 (t, J = 11.34 Hz, 2H), 6.99 (d, J = 8.79 Hz, 2H), 7.10 (d, J = 8.79 Hz, 1H), 7.70 (d, J = 8.61 Hz, 2H), 9.99 (s, 1H), MS (ESI): 579 ($C_{25}H_{19}ClF_3N_4O_7$, $[M + H]^+$). Anal $C_{25}H_{18}ClF_3N_4O_7$. Calcd for: C, 51.87; H, 3.13; N, 9.68. Found: C, 51.78; H, 3.02; N, 9.71%.

4.5.9. (*E*)1-(5-(3,5-Dibromo-2-(2,6-dinitro-4-(trifluoromethyl)-phenoxy)phenyl)-3-(4-fluorophenyl)-4,5-dihydro-1*H*-pyrazol-1-yl)-ethanone (4i). White solid, mp: 199–201 °C. ^{1}H NMR (300 MHz, DMSO) δ: 2.41 (d, J = 18.84 Hz, 3H), 3.77 (s, 2H), 3.83 (d, J = 7.68 Hz, 1H), 5.65–5.70 (m, 1H), 7.01 (s, 1H), 7.30 (t, J = 8.87 Hz, 2H), 7.64 (d, J = 2.19 Hz, 1H), 7.83 (t, J = 8.61 Hz, 2H), 9.79 (s, 1H), MS (ESI): 689 ($C_{25}H_{15}Br_2F_4N_4O_6$, $[M + H]^+$). Anal $C_{25}H_{14}Br_2F_4N_4O_6$. Calcd for: C, 41.76; H, 2.04; N, 8.12. Found: C, 41.78; H, 2.02; N, 8.11%.

4.5.10. (*E*)1-(5-(3,5-Dichloro-2-(2,6-dinitro-4-(trifluoromethyl)-phenoxy)phenyl)-3-(4-fluorophenyl)-4,5-dihydro-1*H*-pyrazol-1-yl)-ethanone (4j). White solid, mp: 213–215 °C. ^{1}H NMR (300 MHz, DMSO) δ: 2.43 (d, J = 2.19 Hz, 3H), 3.79 (d, J = 2.19 Hz, 2H), 3.85 (d, J = 8.87 Hz, 1H), 5.70 (s, 1H), 7.04 (s, 1H), 7.32 (d, J = 8.87 Hz, 2H), 7.67 (t, J = 2.19 Hz, 1H), 7.85 (d, J = 8.87 Hz, 2H), 9.92 (s, 1H), MS (ESI): 601 ($C_{25}H_{15}Cl_2F_4N_4O_6$, $[M + H]^+$). Anal $C_{25}H_{14}Cl_2F_4N_4O_6$. Calcd for: C, 47.94; H, 2.35; N, 9.32. Found: C, 47.78; H, 2.32; N, 9.21%.

4.5.11. (*E*)1-(5-(5-Bromo-2-(2,6-dinitro-4-(trifluoromethyl)-phenoxy)phenyl)-3-(4-fluorophenyl)-4,5-dihydro-1*H*-pyrazol-1-yl)-ethanone (4k). White solid, mp: 215–217 °C. ^{1}H NMR (300 MHz, DMSO) δ: 2.30 (s, 3H), 3.89 (d, J = 8.4 Hz, 2H), 3.95 (s, 1H), 5.75 (s, 1H), 6.79 (t, J = 7.13 Hz, 1H), 7.06 (d, J =

Published on 08 November 2013. Downloaded by St. Petersburg State University on 12/02/2014 16:18:01.

2.13 Hz, 1H), 7.24 (d, J = 2.13 Hz, 2H), 7.75 (d, J = 8.4 Hz, 2H), 9.92 (s, 1H), MS (ESI): 567 ($C_{24}H_{15}BrF_4N_4O_6$, $[M + H]^+$). Anal $C_{24}H_{14}BrF_4N_4O_6$. Calcd for: C, 47.15; H, 2.47; N, 9.17. Found: C, 47.09; H, 2.52; N, 9.11%.

4.5.12. (*E*)1-(5-(5-Chloro-2-(2,6-dinitro-4-(trifluoromethyl)-phenoxy)phenyl)-3-(4-fluorophenyl)-4,5-dihydro-1*H*-pyrazol-1-yl)-ethanone (4l). White solid, mp: 195–197 °C. ^{1}H NMR (300 MHz, DMSO) δ: 2.32 (s, 3H), 4.03 (t, J = 7.13 Hz, 3H), 5.80 (s, 1H), 6.83 (d, J = 9.15 Hz, 1H), 7.10 (d, J = 8.4 Hz, 1H), 7.28 (t, J = 8.78 Hz, 2H), 7.81 (t, J = 7.13 Hz, 2H), 10.00 (s, 1H), MS (ESI): 567 ($C_{24}H_{15}ClF_4N_4O_6$, $[M + H]^+$). Anal $C_{24}H_{14}ClF_4N_4O_6$. Calcd for: C, 50.85; H, 2.67; N, 9.88. Found: C, 50.78; H, 2.62; N, 9.81%.

4.5.13. (*E*)1-(3-(4-Chlorophenyl)-5-(3,5-dibromo-2-(2,6-dinitro-4-(trifluoromethyl)phenoxy)phenyl)-4,5-dihydro-1*H*-pyrazol-1-yl)-ethanone (4m). White solid, mp: 205–207 °C. ^{1}H NMR (300 MHz, DMSO) δ: 2.27 (s, 3H), 3.58 (s, 3H), 6.47 (d, J = 8.4 Hz, 2H), 6.87 (t, J = 2.19 Hz, 1H), 7.17 (d, J = 2.17 Hz, 2H), 7.45 (t, J = 8.61 Hz, 2H), 9.95 (s, 1H), MS (ESI): 705 ($C_{24}H_{15}Br_2ClF_3N_4O_6$, $[M + H]^+$). Anal $C_{24}H_{14}Br_2ClF_3N_4O_6$. Calcd for: C, 40.79; H, 2.00; N, 7.93. Found: C, 40.78; H, 2.02; N, 8.01%.

4.5.14. (*E*)1-(3-(4-Chlorophenyl)-5-(3,5-dichloro-2-(2,6-dinitro-4-(trifluoromethyl)phenoxy)phenyl)-4,5-dihydro-1*H*-pyrazol-1-yl)-ethanone (4n). White solid, mp: 213–215 °C. ^{1}H NMR (300 MHz, DMSO) δ: 2.32 (s, 3H), 3.74–3.84 (m, 3H), 6.78 (d, J = 8.58 Hz, 2H), 6.94 (d, J = 2.19 Hz, 1H), 7.21–7.25 (m, 2H), 7.51 (d, J = 8.61 Hz, 2H), 10.00 (s, 1H), MS (ESI): 617 ($C_{24}H_{15}Cl_3F_3N_4O_6$, $[M + H]^+$). Anal $C_{24}H_{14}Cl_3F_3N_4O_6$. Calcd for: C, 46.66; H, 2.28; N, 9.07. Found: C, 46.78; H, 2.22; N, 9.01%.

4.5.15. (*E*)1-(5-(5-Bromo-2-(2,6-dinitro-4-(trifluoromethyl)-phenoxy)phenyl)-3-(4-chlorophenyl)-4,5-dihydro-1*H*-pyrazol-1-yl)ethanone (4o). White solid, mp: 271–273 °C. ^{1}H NMR (300 MHz, DMSO) δ: 2.32 (s, 3H), 3.76 (s, 1H), 4.02 (d, J = 8.58 Hz, 2H), 6.87 (d, J = 2.37 Hz, 1H), 7.40 (d, J = 2.37 Hz, 1H), 7.51 (d, J = 8.58 Hz, 2H), 7.60–7.65 (m, 1H), 7.78 (d, J = 8.58 Hz, 2H), 7.94 (s, 1H), 9.91 (s, 1H), MS (ESI): 627 ($C_{24}H_{16}BrClF_3N_4O_6$, $[M + H]^+$). Anal $C_{24}H_{15}BrClF_3N_4O_6$. Calcd for: C, 45.92; H, 2.41; N, 8.92. Found: C, 45.88; H, 2.42; N, 8.97%.

4.5.16. (*E*)1-(5-(5-Chloro-2-(2,6-dinitro-4-(trifluoromethyl)-phenoxy)phenyl)-3-(4-chlorophenyl)-4,5-dihydro-1*H*-pyrazol-1-yl)-ethanone (4p). White solid, mp: 275–277 °C. ^{1}H NMR (300 MHz, DMSO) δ: 2.32 (s, 3H), 3.79 (s, 1H), 4.05 (t, J = 2.37 Hz, 2H), 6.93 (d, J = 2.37 Hz, 1H), 7.45 (t, J = 8.4 Hz, 1H), 7.51 (d, J = 8.58 Hz, 2H), 7.68 (s, 1H), 7.81 (t, J = 2.13 Hz, 2H), 7.93 (d, J = 8.58 Hz, 1H), 9.95 (s, 1H), MS (ESI): 627 ($C_{24}H_{16}Cl_2F_3N_4O_6$, $[M + H]^+$). Anal $C_{24}H_{15}Cl_2F_3N_4O_6$. Calcd for: C, 49.42; H, 2.59; N, 9.61. Found: C, 49.38; H, 2.52; N, 9.57%.

4.5.17. (*E*)1-(3-(4-Bromophenyl)-5-(3,5-dibromo-2-(2,6-dinitro-4-(trifluoromethyl)phenoxy)phenyl)-4,5-dihydro-1*H*-pyrazol-1-yl)-ethanone (4q). White solid, mp: 247–249 °C. ^{1}H NMR (300 MHz, DMSO) δ: 2.32 (s, 3H), 3.76 (d, J = 8.58 Hz, 2H), 4.32 (s, 1H), 5.64–5.69 (m, 1H), 7.01 (s, 1H), 7.64–7.73 (m, 5H), 9.76 (s, 1H), MS (ESI): 749 ($C_{24}H_{15}Br_3F_3N_4O_6$, $[M + H]^+$). Anal $C_{24}H_{14}Br_3F_3N_4O_6$. Calcd for: C, 38.38; H, 1.88; N, 7.46. Found: C, 38.41; H, 1.82; N, 7.47%.

4.5.18. (*E*)1-(3-(4-Bromophenyl)-5-(3,5-dichloro-2-(2,6-dinitro-4-(trifluoromethyl)phenoxy)phenyl)-4,5-dihydro-1*H*-pyrazol-1-yl)-ethanone (4r). White solid, mp: 245–247 °C. ^{1}H NMR (300 MHz, DMSO) δ: 2.32 (s, 3H), 3.82 (s, 1H), 4.33 (s, 2H), 5.64–5.69 (m, 1H), 7.01 (d, J = 2.19 Hz, 1H), 7.64–7.73 (m, 5H), 9.76 (s, 1H), MS (ESI): 749 ($C_{24}H_{15}BrCl_2F_3N_4O_6$, $[M + H]^+$). Anal $C_{24}H_{14}BrCl_2F_3N_4O_6$. Calcd for: C, 43.53; H, 2.13; N, 8.46. Found: C, 43.46; H, 2.12; N, 8.47%.

4.5.19. (*E*)1-(5-(5-Bromo-2-(2,6-dinitro-4-(trifluoromethyl)-phenoxy)phenyl)-3-(4-bromophenyl)-4,5-dihydro-1*H*-pyrazol-1-yl)-ethanone (4s). White solid, mp: 255–257 °C. ^{1}H NMR (300 MHz, DMSO) δ: 2.32 (s, 3H), 3.47 (s, 1H), 4.33 (s, 2H), 5.64–5.70 (m, 1H), 6.75 (d, J = 8.79 Hz, 2H), 7.01 (d, J = 2.19 Hz, 1H), 7.64–7.73 (m, 4H), 9.77 (s, 1H), MS (ESI): 671 ($C_{24}H_{16}Br_2F_3N_4O_6$, $[M + H]^+$). Anal $C_{24}H_{15}Br_2F_3N_4O_6$. Calcd for: C, 42.88; H, 2.25; N, 8.33. Found: C, 42.86; H, 2.22; N, 8.37%.

4.5.20. (*E*)1-(3-(4-Bromophenyl)-5-(5-chloro-2-(2,6-dinitro-4-(trifluoromethyl)phenoxy)phenyl)-4,5-dihydro-1*H*-pyrazol-1-yl)-ethanone (4t). White solid, mp: 270–272 °C. ^{1}H NMR (300 MHz, DMSO) δ: 2.33 (s, 3H), 3.80 (s, 1H), 4.34 (s, 2H), 5.61 (s, 1H), 6.84 (d, J = 8.79 Hz, 2H), 7.11 (t, J = 4.29 Hz, 1H), 7.64–7.73 (m, 4H), 10.01 (s, 1H), MS (ESI): 627 ($C_{24}H_{16}BrClF_3N_4O_6$, $[M + H]^+$). Anal $C_{24}H_{15}BrClF_3N_4O_6$. Calcd for: C, 45.92; H, 2.41; N, 8.92. Found: C, 45.86; H, 2.32; N, 8.87%.

4.6. *In vitro* antibacterial activity

The antibacterial activities of the synthetic compounds were tested against two Gram-negative bacterial strains: *E. coli* ATCC 25922 and *P. aeruginosa* ATCC 27853, and also two Gram-positive bacterial strains: *B. subtilis* ATCC 530 and *S. aureus* ATCC 25923, using the method recommended by the National Committee for Clinical Laboratory Standards (NCCLS).

In vitro activities of the compounds were tested in nutrient broth (NB) for bacteria by the two-fold serial dilution method. Seeded broth (broth containing microbial spores) was prepared in NB from 24 h-old bacterial cultures on nutrient agar (Hi-media) at 37 ± 1 °C. The bacterial suspension was adjusted with sterile saline to a concentration of between 1×10^4 and 10^5 CFU. The tested compounds and reference drugs were prepared by two-fold serial dilution to obtain the required concentrations of 50, 25, 12.5, 6.25, 3.125, 1.562, 0.78 and 0.39 μg mL^{-1}. The tubes were incubated in BOD incubators at 37 ± 1 °C for bacteria. The MICs were recorded by visual observations after 24 h (for bacteria) of incubation. Kanamycin B and penicillin were used as standards for antibacterial agents. The observed MICs are presented in Table 2.

4.7. Enzyme inhibition

4.7.1. *S. aureus* DNA gyrase supercoiling. The *S. aureus* DNA gyrase was purified using the method of Blanche *et al.*[30] from a crude extract of *S. aureus* and cultivated with medium B,[31] which was composed of 10 g of polypeptide, 2 g of yeast extract, 8 g of Na_2HPO_4, 2 g of KH_2PO_4, 1.2 g of

 This journal is © The Royal Society of Chemistry 2014

Published on 08 November 2013. Downloaded by St. Petersburg State University on 12/02/2014 16:18:01.

$(NH_4)_2SO_4$, 0.2 g of $MgSO_4$, and 4 g of glucose per liter of distilled water. Supercoiling and deactivation were performed according to the method of Blanche *et al*.[30]

4.7.2. *B. subtilis* DNA gyrase supercoiling. The *B. subtilis* DNA gyrase was purified using the method of Elisha and Walter.[32] Cells were suspended in an equal volume of 25 mM HEPES–KOH (pH 8.0) 100 mM KCl and stored frozen at 70 °C. The frozen cell suspension was thawed and diluted with an equal volume of 25 mM HEPES–KOH (pH 8.0)–0.4 M sucrose–20 mM magnesium acetate–1 mM dithiothreitol–5 mM PMSF. All operations were performed at 0–4 °C. Lysozyme was added to a final concentration, and the mixture was incubated for 2.5 h. One-third volume of 2 M KCl–1.5% Brij was added, and the incubation was continued for 15 min. The lysate was then centrifuged for 90 min using a Ti Rotor. The supernatant was adjusted to a KCl concentration of 0.2 M by dilution with 25 mM HEPES–KOH (PH 8.0)–1 mM dithiothreitol–1 mM EDTA–0.5 mM PMSF–10% ethylene glycol and applied to a column. The column was washed with starting buffer and eluted successively with buffer containing 20 mM ATP–25 mM magnesium acetate–0.2 M KCl, buffer (2 M KCI), and 5 M urea in buffer (0.2 M KCl). Protein-containing fractions were dialyzed against buffer (0.05 M KCI). Supercoiling and deactivation were carried out using the method of Blanche *et al*.[31]

4.8. Safety test

4.8.1. Hemolysis test. Hemolytic activity was assayed using fresh capillary human blood. Erythrocytes were collected by centrifuging the blood three times in chilled phosphate buffered saline (PBS at 4 °C) at 1000*g* for 10 min. The final pellet was resuspended in PBS to give a 2% w/v solution. Using a microtitre plate, 100 μL of the erythrocyte solution was added to dextran, PLL, stearyl-PLL or stearyl-PLL + LDL (1–1000 μg mL^{-1}) in a volume of 100 mL. Samples were then incubated for 3 h and the microtitre plate was then centrifuged at 1000*g* for 10 min and the supernatants (100 μL) transferred into a new microtitre plate. Hemoglobin release was determined spectrophotometrically using a microtitre plate reader (absorbance at 550 nm). Results were expressed as the amount of released hemoglobin induced by the compounds as a percentage of the total. Hemolysis test was tested according to the guide of biological evaluation of medical device (SFDA, China).

4.8.2. Cytotoxicity test. The cytotoxic activity *in vitro* was measured against mouse fibroblast NIH-3T3 cells using the MTT assay. Cells were cultured in a 96-well plate at a density of 5×10^5 cells and different concentrations of compounds were respectively added to each well. The incubation was permitted at 37 °C, 5% CO_2 atmosphere for 24 h before the cytotoxicity assessments. 20 μL MTT reagent (4 mg mL^{-1}) was added per well 4 h before the end of the incubation. Four hours later, the plate was centrifuged at 1200 rcf for 5 min and the supernatants were removed, then to each well was added 200 μL DMSO. The absorbance was measured at a wavelength of 490 nm (OD 490 nm) on an ELISA microplate reader. Three replicate wells were used for each concentration and each assay was measured three times, after which the average IC_{50} value was calculated. The cytotoxicity of each compound was expressed as the concentration of compound that reduced cell viability to 50% (IC_{50}: half maximal inhibitory concentration). The results are summarized in Table 3.

4.8.3. Acute toxicity. Before the acute toxicity experiment, mice were stopped being served food but water remained available for 3 h. The test substances were dissolved in maize germ oil.[33] The preliminary experiment was performed as follows: four dose levels, 100, 500, 2000, and 5000 mg kg^{-1} bodyweight, and three mice for each level were used. We observed the death and evident toxicity within 7 days to determine the general concentration range. Then the administration doses were graded with geometric progression for ease of the calculation of the LD_{50} data. Mice were randomly divided into groups (10 mice per group). Then the mice were weighed and the test substances of different concentrations were administered to mice in varied doses by gavage (0.1–0.2 mL per 100 g). The control groups received maize germ oil only. After the administration, food was withheld for 2 h.

4.9. Docking

The pdb file about the crystal structure of the DNA gyrase (3G75.pdb) was obtained from the RCSB protein data bank (http://www.pdb.org). The molecular docking procedure was performed by using the CDOCKER protocol for the receptor–ligand interactions section of Discovery Studio 3.1 (Accelrys Software Inc., San Diego, CA). Initially both the ligands and the receptor were pretreated. For ligand preparation, the 3D structures of all the steroidal compounds were generated using ChemBioOffice 2010 and optimized using the MMFF 94 method. For enzyme preparation, the hydrogen atoms were added with the pH of the protein in the range of 6.5–8.5. CDOCKER is an implementation of a CHARMm-based molecular docking tool using a rigid receptor.[34] It includes the following steps:

(1) A series of ligand conformations are generated using high temperature molecular dynamics with different random seeds.

(2) Random orientations of the conformations are generated by translating the center of the ligand to a specified position within the receptor active site, and making a series of random rotations. A softened energy is calculated and the orientation is kept when it is less than a specified limit. This process is repeated until either the desired number of low-energy orientations is obtained, or the test times of bad orientations reached the maximum number.

(3) Each orientation is subjected to simulated annealing molecular dynamics. The temperature is heated to a high temperature then cooled to the target temperature. A final energy minimization of the ligand in the rigid receptor using a non-softened potential is performed.

(4) For each of the final conformations, the CHARMm energy (interaction energy plus ligand strain) and the interaction energy alone are figured out. The poses are sorted according to the CHARMm energy and the top scoring (most negative, thus favorable to binding) poses are retained.

Published on 08 November 2013. Downloaded by St. Petersburg State University on 12/02/2014 16:18:01.

CHARMm was selected as the force field. The molecular docking was performed with a simulated annealing method. The heating steps were 2000 with 700 of heating target temperature. The cooling steps were 5000 with 300 cooling target temperature. Ten molecular docking poses saved for each ligand were ranked according to their dock score function. The pose with the highest CDOCKER energy was chosen as the most suitable pose.

Acknowledgements

The work was financed by a grant (no. CXLX13_038) from Jiangsu Ordinary University Graduate Students Scientific Research Innovation Plan of China.

References

1 J. Wang, *et al.*, *Nature*, 2006, **441**, 358–361.
2 M. Leeb, *Nature*, 2004, **431**, 892–893.
3 R. J. Reece and A. Maxwell, *Crit. Rev. Biochem. Mol. Biol.*, 1991, **26**, 335–375.
4 L. Gomez, M. D. Hack, J. Wu, J. J. M. Wiener, H. Venkatesan, A. Santilln, D. J. Pippel Jr., N. Mani, B. J. Motley, S. T. Morrow, K. J. Shaw, R. Wolin, C. A. Grice and T. K. Jones, *Bioorg. Med. Chem. Lett.*, 2007, **17**, 2723–2727.
5 T. Miyamoto, J. Matsumoto, K. Chiba, H. Egawa, K. Shibamori, A. Minamida, Y. Nishimura, H. Okada, M. Kataoka and M. Fujita, *J. Med. Chem.*, 1990, **33**, 1645–1656.
6 T. P. Tran, E. L. Ellsworth, J. P. Sanchez, B. M. Watson, M. A. Stier, H. D. Hollis Showalter, J. M. Domagala, M. A. Shapiro, E. T. Joannides, S. J. Gracheck, D. Q. Nguyen, P. Bird, J. Sharadendu, A. Yip, C. Ha, S. Ramezani, X. Wuc and R. Singh, *Bioorg. Med. Chem. Lett.*, 2007, **17**, 1312–1320.
7 A. Tanitame, Y. Oyamada, K. Ofuji, Y. Kyoya, K. Suzuki, H. Ito, M. Kawasaki, K. Nagai, M. Wachid and J. I. Yamagishi, *Bioorg. Med. Chem. Lett.*, 2004, **14**, 2857–2862.
8 A. A. Bekhita and T. Abdel-Aziem, *Bioorg. Med. Chem.*, 2004, **12**, 1935–1945.
9 A. Tanitame, Y. Oyamada, K. Ofuji, M. Fujimoto, K. Suzuki, T. Ueda, H. Terauchi, M. Kawasaki, K. Nagai, M. Yamagishib and J. I. Wachie, *Bioorg. Med. Chem.*, 2004, **12**, 5515–5524.
10 A. A. Bekhit, H. M. A. Ashour, Y. S. AbdelGhany, A. E.-D. A. Bekhit and A. Baraka, *Eur. J. Med. Chem.*, 2008, **43**, 456–463.
11 X.-H. Liu, B.-F. Ruan, J.-X. Liu, B.-A. Song, L.-H. Jing, J. Li, Y. Yang, X.-B. Qi and H.-L. Zhu, *Bioorg. Med. Chem. Lett.*, 2011, **21**, 2916–2920.
12 R. G. Ridley, W. Hofheinz, H. Matile, C. Jaquet, A. Dorn, R. Masciadri, S. Jolidon, W. F. Richter, A. Guenzi, M. A. Girometta, H. Urwyler, W. Huber, S. Thaithong and W. Peters, *Antimicrob. Agents Chemother.*, 1996, **40**, 1846–1854.
13 D. Y. D. De, F. M. Krogstad, L. D. Byers and D. J. Krogstad, *J. Med. Chem.*, 1998, **41**, 4918–4926.
14 D. Azarifar and H. Ghasemnejad, *Molecules*, 2003, **8**, 642–648.
15 X.-H. Liu, J. Zhu, A.-n. Zhou, B.-A. Song, H.-L. Zhu, L.-S. bai, P. S. Bhadury and C.-X. Pan, *Bioorg. Med. Chem.*, 2009, **17**, 1207–1213.
16 R. N. Comber, R. J. Gray and J. A. Secrist, *Carbohydr. Res.*, 1991, **216**, 441–452.
17 H. J. Boehm, M. Boehringer, D. Bur, H. Gmuender, W. Huber, W. Klaus, D. Kostrewa, H. Kuehne, T. Lübbers, M. K. Nathalie and F. Mueller, *J. Med. Chem.*, 2000, **43**, 2664–2674.
18 T. Lübbers, P. Angehrn, H. Gmunder, S. Herzig and J. Kulhanek, *Bioorg. Med. Chem. Lett.*, 2000, **10**, 821–826.
19 A. Tanitame, Y. Oyamada, K. Ofuji, M. Fujimoto, N. Iwai, Y. Hiyama, K. Suzuki, H. Ito, H. Terauchi, M. Kawasaki, K. Nagai, M. Wachi and J. I. Yamagishi, *J. Med. Chem.*, 2004, **47**, 3693–3696.
20 J. Sun, P. C. Lv, Y. Yin, R. J. Yuan, J. Ma and H. L. Zhu, *PLoS One*, 2013, **8**, e69751.
21 K. L. Kees, J. J. Fitzgerald, K. E. Steimer, J. F. Mattes, B. Mihan, T. Tosi, D. Mondoro and M. L. McCaleb, *J. Med. Chem.*, 1996, **39**, 3920–3928.
22 T. P. Gregory, C. D. Darlene and M. S. David, *Pestic. Biochem. Physiol.*, 1998, **60**, 177–186.
23 S. G. Kucukguzel, S. Rollas, H. Erdeniz, A. C. Kiraz, M. Ekinci and A. Vidin, *Eur. J. Med. Chem.*, 2000, **35**, 761–771.
24 S. M. Ronkin, M. Badia, S. Bellon, A. L. Grillot, C. H. Gross, T. H. Grossman, N. Mani, J. D. Parsons, D. Stamos, M. Trudeau, Y. Wei and P. S. Charifson, *Bioorg. Med. Chem. Lett.*, 2010, **20**, 2828–2831.
25 J. D. MacLowry, M. J. Jaqua and S. T. Selepak, *Appl. Microbiol.*, 1970, **20**, 46–53.
26 F. Smaill and J. Can, *Gastroenterology*, 2000, **14**, 871–875.
27 J.-Y. Lee, K.-W. Jeong, S. Shin, J.-U. Lee and Y. Kim, *Eur. J. Med. Chem.*, 2012, **47**, 261–269.
28 X. He, M. R. Anne, R. D. Umesh, E. K. Glen and A. R. Kevin, *Antimicrob. Agents Chemother.*, 2004, **48**, 3093–3102.
29 P. Kirkpatrick, *Nat. Rev. Drug Discovery*, 2004, **3**, 299–299.
30 F. Blanche, B. Cameron, F. Bernard, L. Maton, B. Manse, L. Ferro, N. Ratet, C. Lecoq, A. Goniot, D. Bisch and J. Crouzet, *Antimicrob. Agents Chemother.*, 1996, **40**, 2714–2720.
31 K. Sato, Y. Inoue, T. Fujii, H. Anoyama, M. Inoue and S. Mitsuhashi, *Antimicrob. Agents Chemother.*, 1990, **34**, 1088–1097.
32 O. Elisha and L. S. Walter, *J. Bacteriol.*, 1982, **151**, 524–535.
33 U.S. National Library of Medicine, Toxicology Data Network (Toxnet), 2011. Available from http://toxnet.nlm.nih.gov/
34 G. S. Wu, D. H. Robertson, C. L. Brooks and M. Vieth, *J. Comput. Chem.*, 2003, **24**, 1549–1562.

 This journal is © The Royal Society of Chemistry 2014